

## BUBBLE ELIMINATION FOR COATING MATERIAL

### Ryushi SUZUKI

Opus System Inc.  
3-35-20 okusawa, Setagayaku, Tokyo  
158-0083, JAPAN  
TEL +81-3-5499-7885  
FAX +81-3-5499-7886  
E-mail: [rsuzuki@opus.co.jp](mailto:rsuzuki@opus.co.jp)

### Yutaka TANAKA

Hosei University  
3-7-2 Kajinocho, Koganeishi, Tokyo  
184-8584, JAPAN  
TEL+ 81-423-87-6133  
FAX +81-42-387-6121  
E-mail: [tanaka@vr.k.hosei.ac.jp](mailto:tanaka@vr.k.hosei.ac.jp)

### Kazuhiko IWAMOTO

Hosei University  
3-7-2 Kajinocho, Koganeishi, Tokyo  
184-8584, JAPAN  
TEL 81-423-87-6133  
FAX 81-42-387-6121  
E-mail: [iwamoto@vr.k.hosei.ac.jp](mailto:iwamoto@vr.k.hosei.ac.jp)

### Kazuyoshi ARAI

Hosei University  
3-7-2 Kajinocho, Koganeishi, Tokyo  
184-8584, JAPAN  
TEL +81-423-87-6133  
FAX +81-42-387-6121  
E-mail: [arai@cm.me.hosei.ac.jp](mailto:arai@cm.me.hosei.ac.jp)

## Abstract

Bubbles in coating color greatly influence the paper quality and coater runnability. It is particularly important technology to remove bubbles for the paper coating industry. Recently, one of the authors has developed a novel device using swirl flow capable of eliminating bubbles and decreasing dissolved gases from fluid. This device is called the "Bubble Eliminator". Using the bubble eliminator will enable the coated products to make better. In this paper performance evaluation of the bubble eliminator is investigated through numerical analysis and visualization of the swirl flow in the device. Pressure distributions in the bubble eliminator are calculated by a three-dimensional numerical analysis in the case of changing conditions of the fluid flow rate. The swirl flow pattern in a transparent bubble eliminator is visualized and processed as digital image by a high-speed video camera system. The results of the flow visualization are compared between experiments and numerical analysis. The performance evaluation of the bubble removal effectiveness is numerically verified.

## Introductions

For all of coater machines, especially for the high-speed short dwell blade coater, bubbles in coating colors may seriously affect the paper quality and the coating operation. They bring about detrimental effect such as skip coating and cratering. In order to obtain high quality coated papers, effective bubble removable is particularly important for high productivity of coating machines and reduction of the environmental load. Bubbles or air in coating materials have been traditionally handled in adding costly chemicals to the coating for reduction of bubbles or air. Recently commercially available mechanical deaeration units with centrifugal force of a cyclone have been theoretically and experimentally reported and practically used in operation of the coater machines [1][2]. Meanwhile for more than a decade, a bubble removable device developed has been applied for many paper coaters [3]. The original type of the bubble removable device has a cylindrical tube for a swirling flow. Figure 1 shows an example photo of the original type of bubble removable device applied for fields of paper coater machines [4]. In 1994, one of the authors has also improved and developed a new type of the bubble elimination device to solve the problems of the cylindrical type of the device, capable of decreasing dissolved gases using swirl flow [5][8]. The principle of the bubble eliminator, which has a tapered tube section, is a little different from the principle of cyclones. This device is called the "Bubble Eliminator"[6]. Simple structure and low pressure drop are features

of the bubble eliminator. Decreasing bubbles in fluids results in to prevent foam build-up. Using the bubble eliminator will enable coating material to improve better quality. Figure 2 shows the bubble eliminator applied for paper coater machines. In our previous study [7], we have reported that the bubble eliminator is useful for removing tiny cavitation bubble from the hydraulic oil for fluid power systems. In the bubble eliminator of designing for the appropriate conditions, a laminar flow with a superimposed swirl creates a minimum pressure region along a central axis and an adverse pressure gradient is generated on a downstream region. A backward force is acted upon bubbles located at the adverse pressure area. The pressure distribution in the bubble eliminator greatly influence the effectiveness of bubble removal.

In this paper performance evaluation of bubble eliminator is studied through visualization and numerical analysis of the swirling flow. The swirling flow patterns in the bubble eliminator are calculated by a three-dimensional numerical analysis for single-phase flow and multi-phase under some fluids conditions. The swirling flow pattern in a transparent bubble eliminator is also visualized and processed as the digital image by the high-speed video camera system. Time variant collected bubbles are presented by numerical simulation and flow visualization.

### **Principle of the Bubble Elimination**

The developed bubble eliminator is able to eliminate bubbles from fluids while flowing in a fluid line. Figure 3 illustrates the principle of the bubble eliminator. The bubble eliminator consists of three elements; an inlet-tube, a tapered-tube, and a straight tube. Liquids with bubbles flow tangentially into the tapered-tube from an inlet ports and form a swirling flow that circulates through the flow passage in the tapered-tube. The swirling flow accelerates and the fluid pressure along the central axis decreases. From the end of tapered-tube, the swirling flow decelerates downstream and the pressure recovers toward the outlet. Small bubbles are trapped and make the large air column in the vicinity of central axis of the swirl near the area where the pressure is lowest. When back pressure is applied at the downstream side of the bubble eliminator, the collected bubbles are ejected through a vent port.

In the previous study [8], it is experimentally confirmed that the bubble eliminator has been able to eliminate bubbles and dissolved gases from the fluid. The swirling flow pattern and the pressure distribution in the tapered-tube chamber of the bubble eliminator greatly influence the effectiveness of the bubble removal in principle.

### **Experimental Investigation**

Figure 4 illustrates an experimental fluid circuit for flow visualization. Working fluid in a 20L reservoir fed by a variable displacement-type piston pump flows to a transparent bubble eliminator. The tapered-tube of the transparent bubble eliminator for flow visualization is made from an acrylic pipe. A needle valve at the pump suction side is used experimentally to introduce air into the fluid circuit. The needle valve is slightly opened and external air is admitted in the fluid circuit for bubbling. A relief valve is set for the purpose of the safety pressure in the pump delivery line. A flow rate is measured by flow meter in the downstream of the fluid circuit. A solenoid-type on-off valve is installed on the vent port side of the bubble eliminator. The time interval of closing the vent valve is adjusted and monitored by a control circuit of the on-off valve. In the usual case the on-off valve is opened, and the trapped and collected bubbles are ejected through the vent line. When the on-off valve is closed, the trapped bubbles make a large air column in a flash time. The high-speed camera (FASTCAM-ultima: maximum recording rate of 4300 frame per second) or the digital video camera is set at a flank of the transparent bubble eliminator. We can observe a growth pattern of the trapped bubbles by the swirling flow at the tapered-tube in the bubble eliminator. Working fluid is kinetic viscosity of the fluid for flow visualization is 42 [mm<sup>2</sup>/s] under 30[°C]. Flow rate set up the condition of between 17[l/min] and 20[l/min].

Figure 5 shows the photographs for the flow visualization by the digital video camera. Bubbles are collected along the central axis. It is experimentally verified that the developed bubble eliminator can collect the bubbles in the working fluid by using the swirling flow. Figure 6 shows the series of the photographs at the flow visualization in swirling flow by the

high-speed video camera. In the initial stage when an elapsed time is 0[s], the on-off valve in the vent line is closed. When the on-off valve is closed, the trapped bubbles are collected at the moment and make a large air column along the central axis of chamber toward downstream. In a series of photographs, it is found that the air column grows up within 0.1[s]. The length from inlet port to the top of the air column is 17.5[mm], 27.0[mm], 34.5[mm], 42.75[mm], and 47.50[mm], respectively in accordance with the elapsed time. The time-dependent growth process of the trapped bubbles is experimentally clarified through the flow visualization.

## Numerical Simulation

The step of our numerical investigation consists of calculating a single-phase flow and a multi-phase flow. The results obtain from the numerical calculation of the single-phase flow are available for an initial condition of the multi-phase flow analysis. The swirling flow pattern, the velocity profile and the pressure distribution in the bubble eliminator are calculated by three-dimensional numerical analysis for incompressible viscous fluid. In the multi-phases flow analysis, it is assumed that small air particles are mixed with the fluid in the bubble eliminator. The diameter of the mixed particles keeps at a constant value of 1[mm]. A surface tension and buoyancy of the air particle is neglected. Time variant distributions of the collected air particles are calculated by the results of single-phase analysis for the initial values. A time interval of numerical simulation for the multi-phase flow analysis is 0.1[ms].

Figure 7 shows the typical five definition blocks for the numerical analysis of the bubble eliminator. The overall apparatus for the bubble eliminator is Inlet port, Peripheral inlet tube, Tangential inlet ports, Tapered-tube, and Downstream tube. The two tangential inlet port regions are divided into smaller rectangles to account for the velocity and pressure value changes. There are 900 cells on the x-y plane of the tapered-tube divided by use of the boundary-fit coordinate. The tapered-tube and downstream tube regions are non-uniformly divided into 55 cells along the z-axis. The number of total cells for the configuration, including the peripheral inlet tube and inlet port, has 81000 cells. We perform a three-dimensional flow analysis of an incompressible viscous fluid using the commercially available numerical calculation software, RFLOW (Rflow Co. Ltd). The basic equations for the numerical analysis consist of the equation of continuity, the equations of motion and energy equation. The basic equations are discretized by the finite volume method using boundary-fit coordinates and are solved by the successive over-relaxation (SOR) method.

## .Results and Discussions

We investigate influence in the bubble eliminator in the case of difference of the tapered tube for the straight one. The fluid conditions have the kinetic viscosity of  $0.3 \text{ cm}^2/\text{s}$  and the density of  $857 \text{ kg}/\text{m}^3$ , respectively. The numerical simulation has been performed under the test conditions of flow rate at  $333 \text{ cm}^3/\text{s}$ . In this case, the average velocity at the outlet side of the downstream tube is  $1 \text{ m}/\text{s}$  and the Reynolds number is 700.

The typical results of the calculated pressure distribution across a longitudinal section for the two types of the inlet chamber are illustrated in Figure 8. The numerical results clearly indicate that the tapered type of the inlet chamber has large pressure gradients along a radius direction. There is a minimum pressure region near the center of the swirl flow. The pressure gradient is sustained axially along the flow tube, so that the bubbles are collected and trapped at the location not far from the center of the inlet section. In the contrary, the straight type of the inlet chamber has a slightly pressure gradient and there is no minimum pressure region. Since the radius of the swirl flow gradually becomes shorter in the tapered-tube, it is easier for moving the bubbles to reach the center. In other words, the centrifugal effect and the radial pressure gradient become larger as the working fluid flows to the downstream side of the tapered-tube.

A pressure distribution along the central axis of the bubble eliminator is shown in Figure 9 All the pressure data is plotted as the end of the downstream tube zero. The pressure at the center of the swirl continuously decreases as the working fluid flows to the downstream side. In the tapered type chamber, there is a minimum pressure point at a close end of the

tapered-tube. Subsequently, the pressure makes a gradual recovery at the center of the adjoining straight downstream tube, because the velocity of the swirl flow is decelerated by the viscosity of the working fluid. The pressure distribution such as described in foregoing drive the bubbles collected at the center to move toward a certain location, usually near the downstream end of the tapered-tube.

The original type bubble eliminator developed by the author had no tapered chamber. The original bubble eliminator had only a straight cylindrical chamber employing the swirl flow. In the straight type bubble eliminator, it is impossible to eliminate bubbles when the flow rate is low. It was because a decrease of flow rate caused a decrease of the swirl velocity as well as a decrease of the pressure gradient along the axis. It is numerically clarified that the pressure gradient in the straight type chamber is lower than that in the tapered type as shown in Figure 8 and Figure 9. The effectiveness of the modified type is numerically demonstrated.

Furthermore, we investigate influence in the bubble eliminator in the case of the different conditions of the flow rate. The numerical simulation has been performed for conditions of fluids having kinetic viscosity of  $30[\text{mm}^2/\text{s}]$ , a density of  $857[\text{kg}/\text{m}^3]$  and flow rate conditions of 10, 20, 30[l/min]. For the flow rate of 20[l/min], the outlet side of the downstream tube has an average viscosity of 1[m/s] and the Reynolds number of 700.

Figure 10 shows that pressure distributions along the central axis of the bubble eliminator are plotted. All pressure data is plotted from the reference at the end of the downstream tube. The pressure at the center of the swirl continuously decreases as the fluid flows downstream. There are minimum pressure points of a close end the tapered-tube. After that, the pressure makes a gradual recovery at the center of the adjoining straight downstream tube, because the velocity of the swirl flow is decreased by the viscosity of the fluid. The recovery pressure gradient in case of the 30[l/min] becomes larger than in one of flow rate 10, 20 [l/min]. The recovery pressure gradient depends on the flow rate of fluid. The pressure distribution drives the light particles such as bubbles to move toward the area of the lowest pressure.

The content ratio of the air particle under the kinetic viscosity of  $30[\text{mm}^2/\text{s}]$ , along the central axis of the bubble eliminator is plotted in Figure 11. The content ratio at the center of the swirl continuously increases as the fluid flows downstream. There is a maximum value at the downstream end point of the tapered-tube. The maximum value of the content ratio of the air particle decreases in accordance with the flow rate of fluid. In this numerical analysis, air particles are regarded as a solid ball which will not mix or collapse, occupying 53 percentage volume of cube having each side as same as a diameter of the particles. Then 53 percentage of air content ratio becomes maximum efficiency of bubble elimination and in case of 30[l/min], 53 percentage of air content ratio of the data means the highest performance.

Figure 12 illustrates the typical numerical results of the percentage of the air content for the multi-phase flow analysis under the flow rate condition of 10, 20, 30[l/min] and the kinetic viscosity of  $30[\text{mm}^2/\text{s}]$ . The distribution of content ration of air particles is demonstrated after 0.05 seconds from the start of the fluid inflow as example of the multi-phase flow analysis. In the initial stage when an elapsed time is 0[s], the fluid contains 3-percentage air particle by volume all over the blocks. The air particles have been collected near the end of the tapered-tube and a column of the air particles has grown up near the central axis of the tube to downstream.

### **Comparison between Experiments and Numerical Analysis**

Figure 13 shows the length of air column comparing to the results of numerical analysis and the experiment of the flow visualization. The length of air column in the case of the numerical analysis is defined as the length between the inlet port and the point of the largest air content ratio at each time obtained from Figure 10. The trapped bubbles behavior of numerical analysis are qualitatively in good agreement with the experimental results of the flow visualization. It is numerically verified that the bubble eliminator collects bubbles effectively near the end of tapered-tube.

## **Conclusions**

In this paper, performance evaluation of the bubble eliminator is investigated through the numerical analysis and flow visualization of swirl flow. As the results of the numerical analysis, the pressure distribution of the device for the swirl flow has a large influence on the performance of the bubble eliminator. The experimental results of the flow visualization are qualitatively in good agreement with the results of numerical analysis. Numerical analysis is one of the effective means to study behavior of the swirl flow in the bubble eliminator. As we have examined in this paper, the efficiency of the bubble elimination can be calculated by means of numerical simulation for a certain bubble eliminator of appropriate design, for the given parameters of the fluid density, viscosity, flow rate and bubble diameter.

Although numerical analysis for actually applied coating colors is not part of this investigation, we are able to carry out the calculation of bubble removal effectiveness for the given fluids of non-Newtonian properties when an equation involving the non-Newtonian model is derived by means of measuring Brookfield viscosity.

We may look forward to solving the problems that have been caused by the entrained bubbles in coating materials by employing the bubble eliminator.

## **Acknowledgments**

The numerical calculations were performed at the Computational Science Research Center (CSRC) of Hosei University. The authors acknowledge with thanks the encouragement received from the staffs of the CSRC as well as the facilities of computations. The authors also wish to thank the staff at Rflow Co. Ltd. for their technical suggestion on the numerical software.



Figure1 Bubble elimination device  
Flow rate 2500 [L/min]

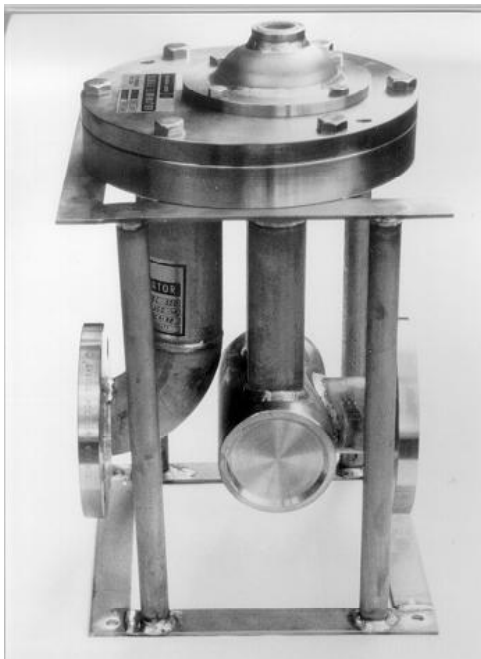


Figure 2 Bubble Eliminator for paper coaster machine  
Flow ratio 300 [L/min].

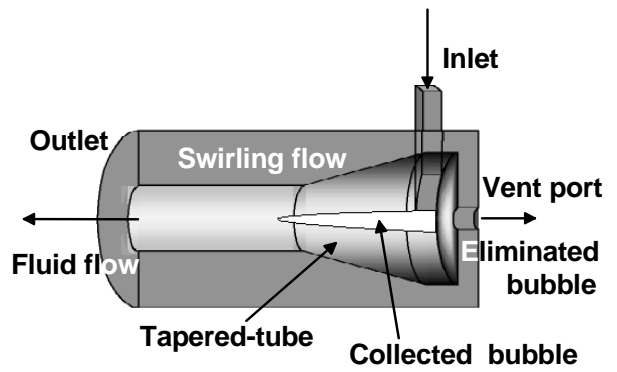


Figure 3 Principle of the bubble eliminator

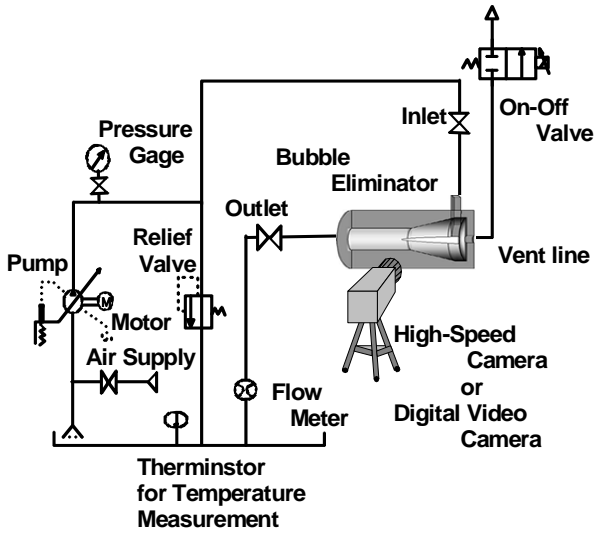


Figure 4 Experimental hydraulic circuit for flow visualization



Collected bubbles

Figure 5 Flow visualization by Digital video camera

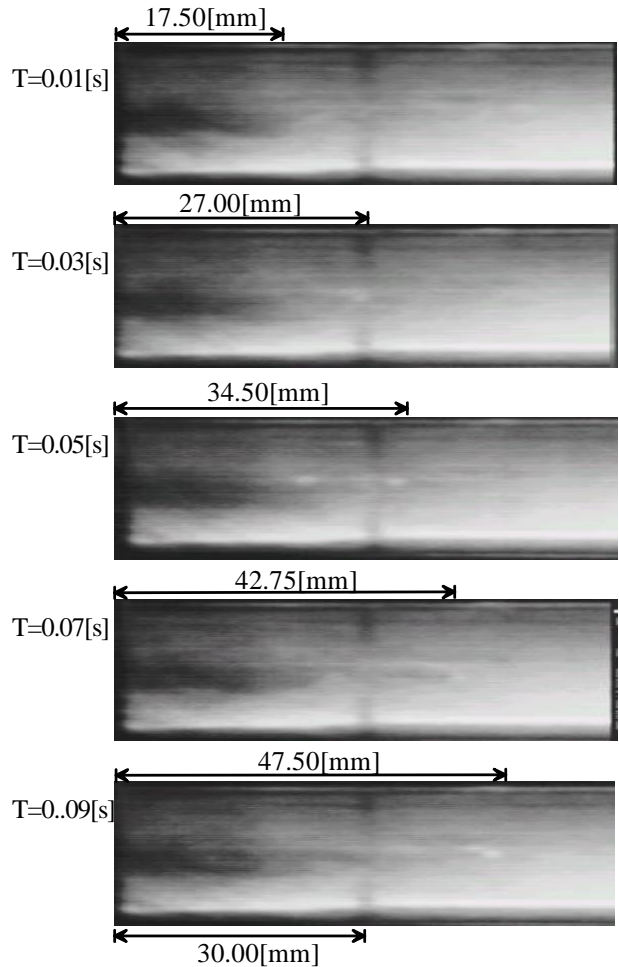


Figure 6 Flow visualization of trapped bubbles by high-speed camera

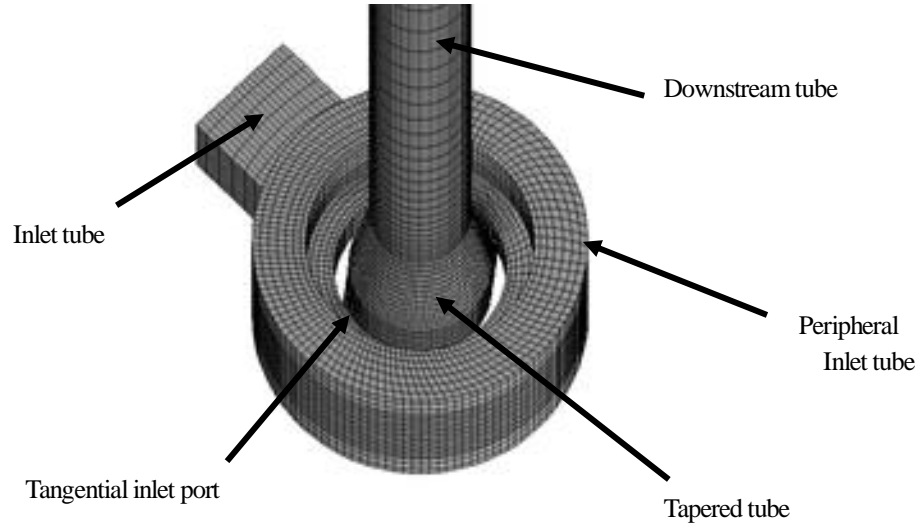


Figure 7 Definition of Blocks for Numerical Analysis

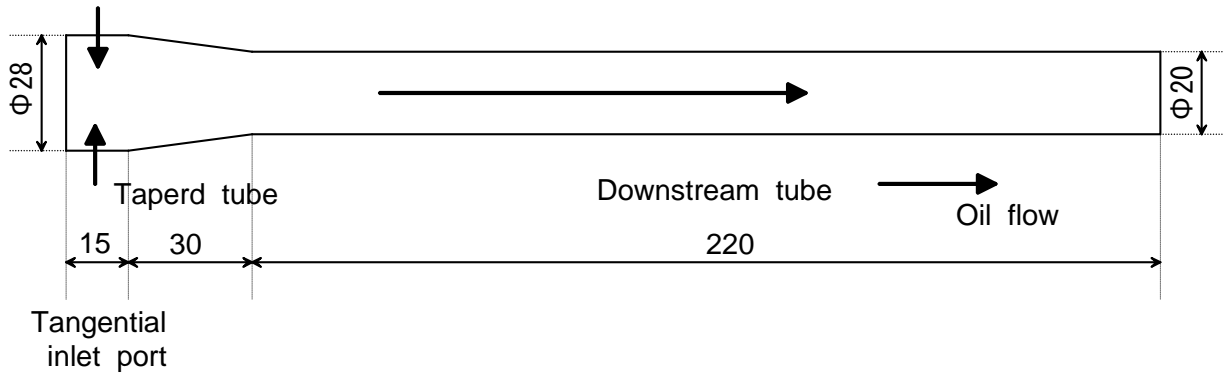


Figure 8(a) Geometry of bubble eliminator

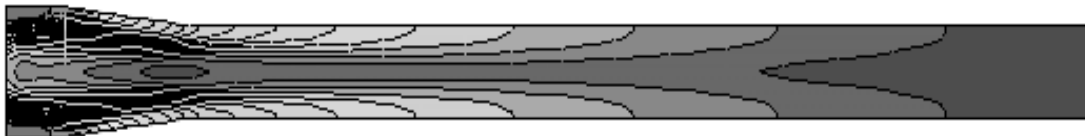


Figure 8(b) Pressure contours for tapered type

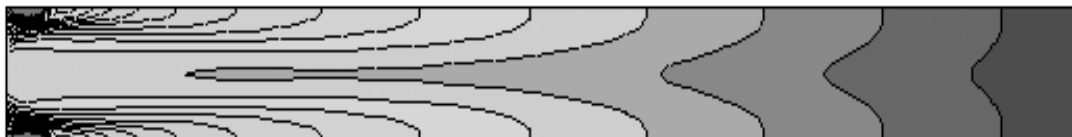


Figure 8(c) Pressure contours for straight type



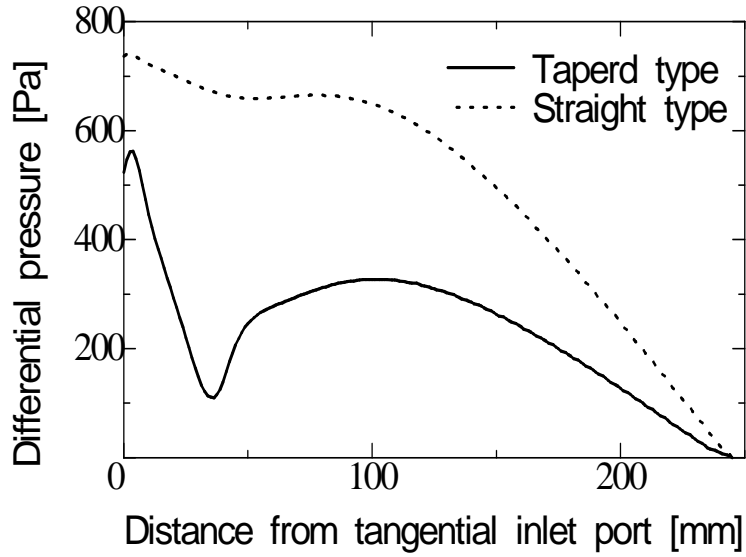


Figure 9 Pressure distribution along central axis

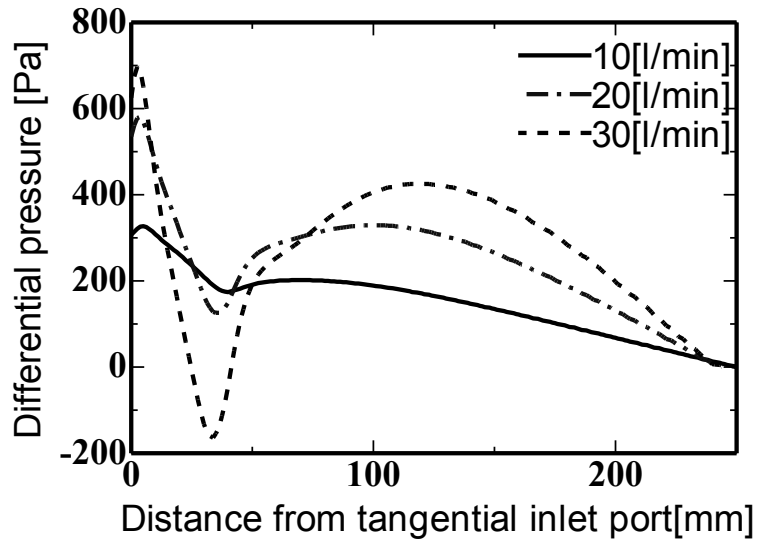


Figure 10 Pressure distribution along central axis for flow rate

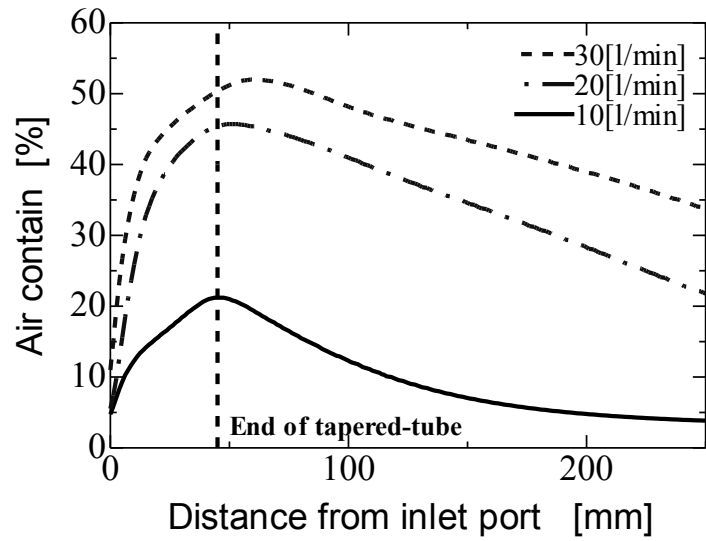


Figure 11 Air particle content along central axis for flow rate

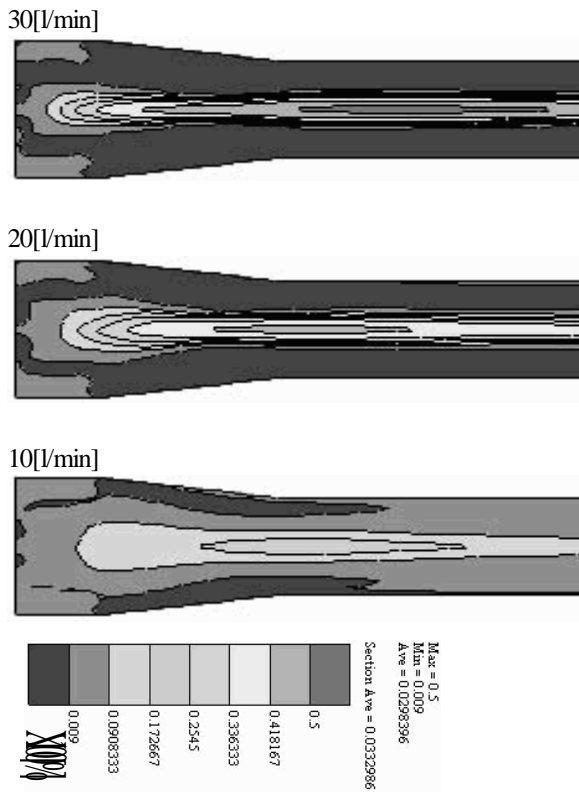


Figure 12 Air particle content time=0.05sec

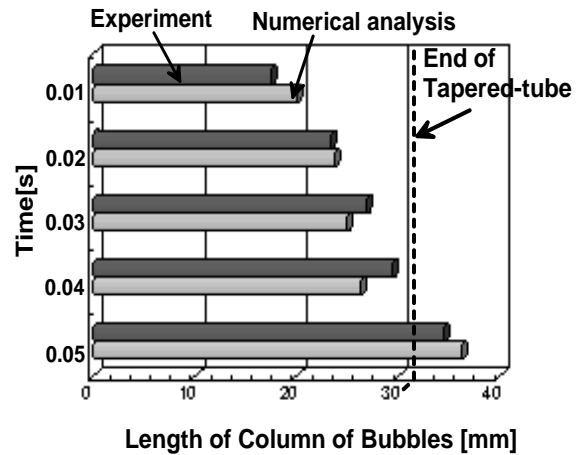


Figure 13 Comparison of flow visualization of the results of experiment and numerical analysis

## References

- [1] Robert Urscheler, "Evaluation of air removal methods in coating colors", TAPPI Coating Conference Proceedings, 1999
- [2] Steve Kaepke, Tapio Jarvensiva "Application of mechanical deaeration to a short dwell blade coater", TAPPI Coating Conference and Trade Fair Proceedings, 2000
- [3] Suzuki, R., "Bubble Eliminator," J. Japan Hydraulics and Pneumatics Soc., 25-3, 1994, 340/345. (in Japanese)
- [4] U.S Patent No, 4585465
- [5] U.S Patent No, 4643746
- [6] U.S Patent No. 5240477
- [7] Suzuki, R., Tanaka, Y., Yokota, S. "Reduction of Oil Temperature Rise by Use of a Bubble Elimination Device in Hydraulic Systems, J. Society of Tribologists and Lubrication Engineers, 54-3, 1998, 23/27
- [8] Suzuki, R., Yokota, S., "Bubble Elimination by Use of Swirl Flow", IFAC Int. Workshop on Trends in Hydraulic and Pneumatic Components and Systems, Poster Paper 2, 1994.